AD A136 310 X-RAY TOPOGRAPHIC MEASUREMENTS OF STRAIN FIELDS(U) 1/1
ILLINOIS UNIV AT URBANA DEPT OF METALLURGY AND MINING
ENGINEERING S R STOCK ET AL. AUG 83 N00014-83-K-0468
UNCLASSIFIED F/G 20/2 NL

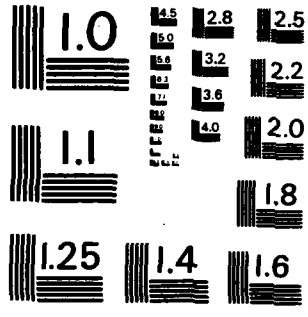

MICROCOPY RESOLUTION TEST CHART
NATIONAL BUREAU OF STANDARDS - 1963 - A

SECURITY CLASSIFICATION OF THIS PAGE (When Data Entered)

10

REPORT DOCUMENTATION PAGE

READ INSTRUCTIONS BEFORE COMPLETING FORM

1. REPORT NUMBER	2. GOVT ACCESSION NO. / 3. RECIPIENT'S CATALOG NUMBER
4. TITLE (and Subtitle): X-Ray Topographic Measurements of Strain Fields	5. TYPE OF REPORT & PERIOD COVERED: Technical Report 6. PERFORMING ORG. REPORT NUMBER
7. AUTHOR(s): S.R. Stock, Haydn Chen and H.K. Birnbaum	8. CONTRACT OR GRANT NUMBER(s): USN 00014-83-K-0468
9. PERFORMING ORGANIZATION NAME AND ADDRESS: University of Illinois, Dept. of Metallurgy and Mining Engineering, Urbana, IL 61801	10. PROGRAM ELEMENT, PROJECT, TASK AREA & WORK UNIT NUMBERS
11. CONTROLLING OFFICE NAME AND ADDRESS: Office of Naval Research, Clark St., Chicago, IL	12. REPORT DATE: August, 1983 13. NUMBER OF PAGES: 9
14. MONITORING AGENCY NAME & ADDRESS (if different from Controlling Office): Office of Naval Research, Arlington, VA	15. SECURITY CLASS. (of this report): unclassified 15a. DECLASSIFICATION/DOWNGRADING SCHEDULE

16. DISTRIBUTION STATEMENT (of this Report)

This document is unclassified. Reproduction and distribution for the purpose of the U.S. government is permitted.

This document has been approved for public release and sale; its distribution is unlimited.

17. DISTRIBUTION STATEMENT (of the abstract entered in Block 20, if different from Report)

18. SUPPLEMENTARY NOTES

DTIC ELECTE DEC 23 1983 A

19. KEY WORDS (Continue on reverse side if necessary and identify by block number)

X-ray topography
Hydrides
Niobium hydride

20. ABSTRACT (Continue on reverse side if necessary and identify by block number)

This report describes a new technique which allows the determination of strain components in solids with a spatial resolution of about 10 micrometers. The method uses x-ray topography and may be applied to specimens which have relatively high dislocation contents. The technique may be used for thin specimens as well as relatively thick ones.

DD FORM 1 JAN 73 1473 EDITION OF 1 NOV 65 IS OBSOLETE
S/N 0102-LF-014-6601

SECURITY CLASSIFICATION OF THIS PAGE (When Data Entered)

A136310

DTIC FILE COPY

X-RAY TOPOGRAPHIC MEASUREMENTS OF STRAIN FIELDS

S.R. Stock, Haydn Chen and H.K. Birnbaum
University of Illinois at Urbana-Champaign
Department of Metallurgy and Mining Eng.
Urbana, IL 61801

Technical Report
August 1983

Office of Naval Research
USN 00014-83-K-0468

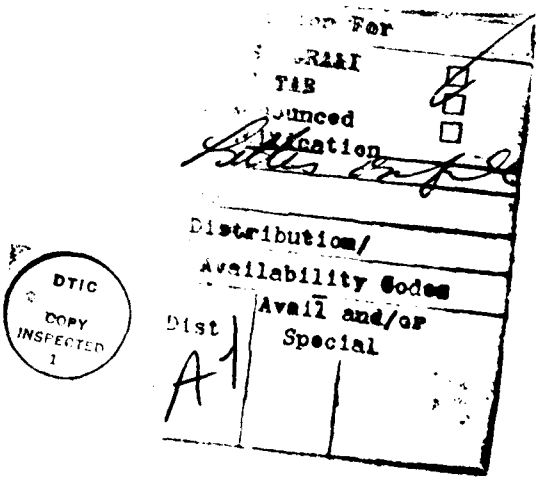

This document is unclassified. Reproduction and distribution for any purpose of the U.S. government is permitted.

88 09 07 133

X-RAY TOPOGRAPHIC MEASUREMENT OF STRAIN FIELDS

S.R. Stock*, Haydn Chen and H.K. Birnbaum

Department of Metallurgy and Mining Engineering
University of Illinois at Urbana-Champaign
Urbana, IL 61801 USA

INTRODUCTION

X-ray diffraction topography offers a unique combination of advantages for imaging dislocations and accumulated plastic deformation in single crystals. Its strain sensitivity and penetrating power are greater than that of electron microscopy, and topography can be used non-destructively to examine a single specimen many times during the course of an experiment. These attributes combine with the limit in attainable magnification to make topography most useful for characterizing crystals with low dislocation densities. With the advent of synchrotron radiation sources and of rapid imaging systems for laboratory sources, the emphasis is shifting from characterization studies to dynamic, in-situ observation of experiments. In heavily deformed crystals, equi-inclination contours (analogues to bend contours in electron microscopy) have been noted[1] although no quantitative use of the angular information implicit in a set of contours has been made.

The purpose of this paper is to use sets of equi-inclination contours (EIC) to determine the components of strain around a strain center about which individual defects cannot be resolved. Analytic methods are developed for both the monochromatic and synchrotron white radiation sources. Some preliminary results are reported for a precipitate of β-NbH in a niobium single crystal.

---

*Now at the Dept. of Mat. Sci. & Eng., Northwestern Univ., Evanston, IL 61201, USA.

Reproduced from best available copy.

RELATIONSHIP BETWEEN THE STRAIN TENSOR AND THE ROTATION REQUIRED FOR DIFFRACTION AT DIFFERENT POINTS IN A CRYSTAL

Consider a strain center which deforms a thin, ribbon-like single crystal. A rectilinear coordinate system with its origin at the strain center may be defined with $\underline{x}_2$ normal to the largest face of the crystal (Fig. 1). Diffraction from planes normal to axis $\underline{x}_i$, denoted by P_i, will be considered for the case of a parallel, spatially-broad monochromatic beam of x-rays. Displacement of atoms from their positions prior to the deformation is given by u_i which are related to the strain tensor by $\varepsilon_{ij} = 1/2(\partial u_i/\partial x_j + \partial u_j/\partial x_i)$. Variation in the interplanar spacing or in the orientation of the diffracting planes, will limit diffraction to a portion of the specimen. Only deformation with components normal to P_i will be sensible, however, and only changes in the displacement u_i will change the diffraction conditions. The change in the displacement across a unit volume element, $\partial u_i/\partial x_j$ is related to the angular change in diffraction conditions, i.e. to $\Delta\omega_i^k(\ell,\ell+1)$, the rotation required to align a new region for diffraction. The superscript k defines the rotation axis $\underline{x}_k$, the subscript i gives the diffraction plane P_i and the arguments ℓ and $\ell+1$ identify the spatial positions of the two volumes of material aligned for diffraction.*

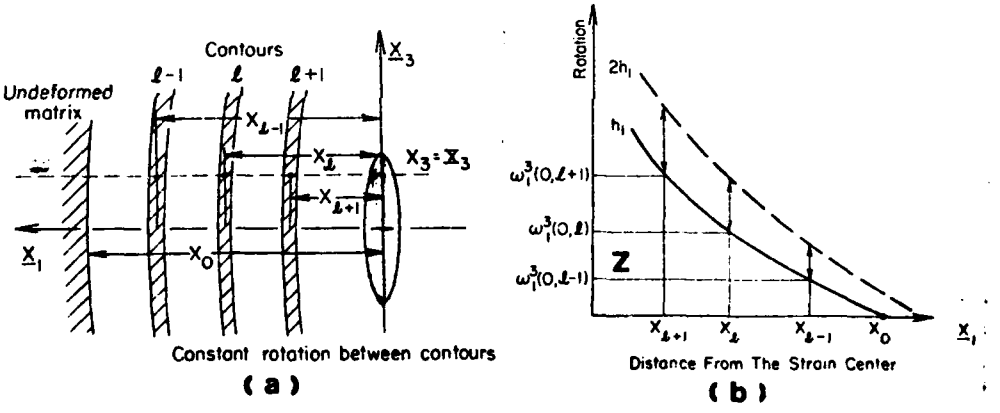

Fig. 1 Schematic diagram of the equi-inclination contour analysis. (a). The contour position on a topograph is shown at distance X_ℓ from the strain center for a rotation of ω_ℓ from the undeformed region of the single crystal. (b). The resulting relationship between X_ℓ and ω_ℓ is plotted for results obtained from topographs taken with diffraction vectors h_1 and $2h_1$.

Since the derivation of the equation relating $\Delta\omega_i^k$ and $\partial u_i/\partial x_j$

*The rotation axis $\underline{x}_k$ is that normally used in x-ray topography; $\underline{x}_1$ and $\underline{x}_3$ for diffraction from P_3 and P_1, respectively, in transmission and either $\underline{x}_1$ or $\underline{x}_3$ for diffraction from P_2 in reflection.

is the same for diffraction from each P_l, only that from P_l will be explicitly considered. Of the terms $\partial u_l/\partial x_j$, $\partial u_l/\partial x_l$ is a dilational strain and $\partial u_l/\partial x_2$ and $\partial u_l/\partial x_3$ are components of shear strains. The total rotation $\Delta\omega_l$, is, therefore, composed of separate contributions from the variation in each of the terms $\partial u_l/\partial x_j$. The form of the contributions to $\Delta\omega_l^k$ are well known[1,2], but the presentation of the particular formulism used here is necessary to understand the analysis.

The change in the Bragg angle $\Delta\theta_D$ from the varying dilational field is related to the change in $\partial u_l/\partial x_l$ from position ℓ to $\ell+1$ through the differential form of Bragg's law:

$$\Delta d/d_o = -\Delta\theta_D \cot\theta_o = \Delta\varepsilon_{11} \equiv \Delta\partial u_l/\partial x_l(\ell,\ell+1), \qquad (1)$$

where $\Delta d = (d_{\ell+1}-d_o) - (d_\ell - d_o)$ and d_o, d_ℓ and $d_{\ell+1}$ are the d-spacings far from the strain center (i.e. in the undeformed state), at ℓ and at $\ell+1$, respectively; $\Delta\theta_D = \theta_{\ell+1}-\theta_\ell$ and θ_o, θ_ℓ and $\theta_{\ell+1}$ are the Bragg angles of the undeformed crystal, at ℓ and at $\ell+1$, respectively.

The shear terms, $\partial u_l/\partial x_2$ and $\partial u_l/\partial x_3$ represent tilting about axes $\underline{x_3}$ and $\underline{x_2}$, respectively. With the experimental rotation axis $\underline{x_3}$, the relationship of the terms $\partial u_l/\partial x_2$ and $\partial u_l/\partial x_3$ to the rotation required to orient region $\ell+1$ for diffraction will be quite different. The contribution of $\partial u_l/\partial x_2$ is trivial to calculate: the angle $\Delta\theta_{S1}$ through which the crystal must be rotated is simply the difference in the amount of tilting at two positions:

$$\Delta\theta_{S1}(\ell,\ell+1)\ (\text{rad.}) = \partial u_l/\partial x_2(\ell+1) - \partial u_l/\partial x_2(\ell) \equiv \Delta\partial u_l/\partial x_2. \qquad (2)$$

Limitation of space precludes detailed consideration of the geometry required to relate the variation in $\partial u_l/\partial x_3$ to the rotation $\Delta\theta_{S2}$; the details will appear elsewhere. Here we will only note that the complication arises because the axis about which changes in $\partial u_l/\partial u_3$ occur is $\underline{x_2}$ while the axis of rotation used to produce EIC in the experiment is $\underline{x_3}$. The equation

$$\sin\theta_o = \sin(\theta_o + \Delta\theta_{S2})\cos\gamma \qquad (3)$$

relates $\Delta\theta_{S2}$ and $\gamma = \Delta\partial u_l/\partial x_3(\ell,\ell+1)$. Before writing the expression for $\Delta\omega_l^3(\ell,\ell+1)$, it is informative to consider the magnitude of the rotations arising from each term. Assuming that each of the derivatives $\partial u_l/\partial x_j$ has a value of 0.01 and that $\theta_o = 12.4°$ ($\underline{g} = [200]$ for niobium with Mo K_α radiation), the rotations $\Delta\theta_D$, $\Delta\theta_{S1}$ and $\Delta\theta_{S2}$ are 450, 2100 and 2.2 seconds of arc, respectively. The contribution of $\Delta\partial u_l/\partial x_3$ is so small that it may be ignored, and one may write

$$\Delta\omega_l^3\ (\text{rad}) = -\Delta\partial u_l/\partial x_l(\ell,\ell+1)\tan\theta_o + \Delta\partial u_l/\partial x_2(\ell,\ell+1)\ . \qquad (4)$$

This expression may be generalized for diffraction from P_i and rotation about rotation axis $\underline{x}_k$, leading to

$$\Delta\omega_i^k \text{ (rad)} = -\Delta\partial u_i/\partial x_i(\ell,\ell+1) \tan\theta_o + \Delta\partial u_i/\partial x_j(\ell,\ell+1) \qquad (5)$$

with the subscript j denoting the third reference direction $\underline{x}_j$ which is perpendicular to both $\underline{x}_i$ and $\underline{x}_k$.

X-RAY TOPOGRAPHY AND THE MEASUREMENT OF THE COMPONENTS OF STRAIN

In x-ray topographs of elastically deformed crystals or those containing an excess dislocation density of one sign, diffraction of monochromatic x-rays produces narrow bands of darkening, termed equi-inclination contours. By multiple exposure of a single piece of film or by a set of singly exposed emulsions, the position of the equi-inclination contour may be mapped as a function of rotation. Characteristic radiation or monochromatized synchrotron radiation may be used to produce the equi-inclination contours. Similar contours (termed absorption edge contours) may be produced with synchrotron white radiation by orienting the deformed crystal so that the range of wavelengths selected encompasses that of the absorption edge of an element of the specimen crystal.

The relationship between equi-inclination or absorption edge contours to strains (Eq. 5) is discussed using Fig. 1 which schematically shows a number of contours recorded between the strain center and the portion of the crystal to which the strain field does not extend. Since transmission topography averages the strain over the thickness of the specimen, only the two-dimensional variation in strain is measured, i.e., $\partial u_i/\partial x_i(x_1,x_3)$. Given constant rotation between contours, it is simple to determine the cumulative rotation from the undeformed region to the position of the ℓth contour $\omega_i^k(\ell)$. The separation between each contour and the strain center X_ℓ is measured along $\underline{x}_i$, the direction normal to the diffraction planes P_i if the usual rotation axis $\underline{x}_k$ is used.* In the example shown in Fig. 1a for diffraction from P_i and rotation about the axis $\underline{x}_k$, $\omega_i^k(\ell)$ and X_ℓ may be measured for each contour along each line $\underline{x}_k = c$ and ω_i^k may be plotted as a function of $\underline{x}_i$ (Fig. 1b). By taking the differences with respect to the position of zero strain, Eq. 5 becomes

$$\omega_i^k(x_i,x_k=c) = -\partial u_i/\partial x_i(x_i,x_k=c) \tan\theta_o + \partial u_i/\partial x_i(x_i,x_k=c). \qquad (6)$$

*One must allow for foreshortening of the diffracted image which can be significant. One does not need to correct for the differences in diffraction angle at different contours, however, as the shift in contour positions from this source is insignificant.

The individual terms $\partial u_i/\partial x_i$ and $\partial u_i/\partial x_j$ cannot be separated based solely upon Eq. 6 and a single plot of cumulative rotations vs. position.

The required additional information may be obtained by carrying out the above procedures for the first and higher order reflections from diffraction planes P_i (represented by diffraction vectors h_i and $2h_i$). The two rotation vs. distance curves which result due to the difference in tan θ_o are shown as solid and dashed lines in Fig. 1b for measurements taken with h_i and $2h_i$, respectively. The difference in cumulative rotation at X_ℓ between the two measurements corresponds to

$$\omega_i^k(x_i,x_k=c)\Big|_{2h_i} - \omega_i^k(x_i,x_k=c)\Big|_{h_i} = \partial u_i/\partial x_i(x_i,x_k=c)(\tan\theta_o^{h_i} - \tan\theta_o^{2h_i}) \quad (7)$$

allowing determination of $\partial u_i/\partial x_i(x_i,x_k=c)$ and $\partial u_i/\partial x_j(x_i,x_k=c)$. Values of $\partial u_i/\partial x_i(x_i,x_k)$ and $\partial u_i/\partial x_j(x_i,x_k)$ may be found by repeated use of Eq. 7 for contours intersecting various x_k. This approach allows the following terms to be determined as a function of position (x_1,x_3): for diffraction plane P_1 and rotation axis $\underline{x}_3$, $\partial u_1/\partial x_1$ and $\partial u_1/\partial x_2$ are measured; for diffraction plane P_3 and rotation axis $\underline{x}_1$, $\partial u_3/\partial x_3$ and $\partial u_3/\partial x_2$ are measured and for diffraction plane P_2 and rotation axis $\underline{x}_1$ or $\underline{x}_3$, $\partial u_2/\partial x_2$ and $\partial u_2/\partial x_3$ or $\partial u_2/\partial x_1$ are measured.

The strain tensor is not completely defined by these measurements, however, as $\partial u_1/\partial x_3$ and $\partial u_3/\partial x_1$ remain to be determined. For a thin specimen, plane stress conditions apply but add no information which helps determine $\partial u_1/\partial x_3$ and $\partial u_3/\partial x_1$. Use of additional rotation axes are required if these terms are to be measured. For diffraction from P_1 (required for determination of $\partial u_1/\partial x_3$), the appropriate rotation axis is $\underline{x}_2$. Terms $\partial u_1/\partial x_1$ and $\partial u_1/\partial x_2$ contribute negligibly to the rotation $\Delta\omega_1$, and only $\partial u_1/\partial x_3$ has a significant effect. For $\partial u_3/\partial x_1$, diffraction from P_3 and rotation about $\underline{x}_2$ is required; $\partial u_3/\partial x_3$ and $\partial u_3/\partial x_2$ produce no contribution.

Instead of using diffraction from first and higher order planes, one may use two or more wavelengths and a single diffraction vector for the analysis. This method is particularly useful when tunable synchrotron radiation is utilized. Another alternative is to use diffraction vectors h_i and $-h_i$, i.e. exchange entrance and exit sides of the specimen. The dilational and shear components will produce rotations which will add in one case and be of the opposite sense in the other. Measurements of cumulative rotation vs. distance for different entrance sides (diffraction vectors h_i and $-h_i$) result in a difference given by

$$\Delta\omega_i^k(h_i) - \Delta\omega_i^k(-h_i) = -2\Delta\ \partial u_i/\partial x_i \tan\theta_o^{h_i}. \quad (8)$$

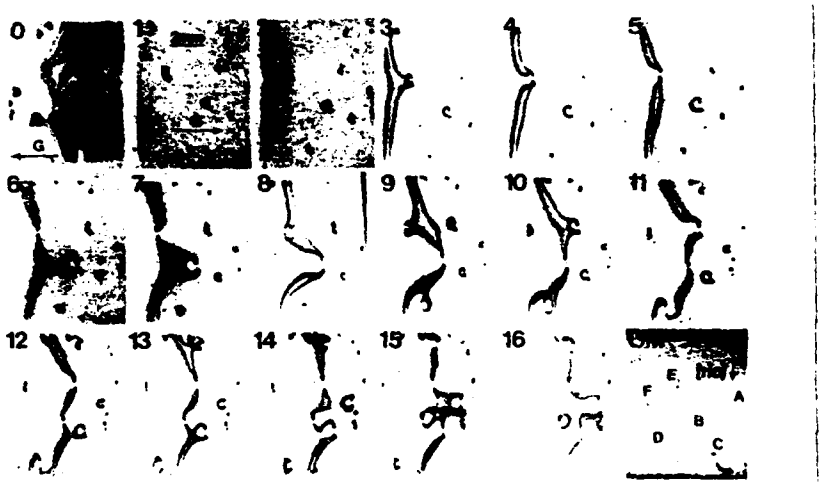

Fig. 2 A composite of topographs taken with $\underline{g}$ = [002] and with the crystal rotated 140" about axis [$\bar{1}$10] between exposures. Plates 0 and OM show a multiple exposure topograph of the equi-inclination contours and an optical micrograph of the hydride positions in the crystal, respectively.

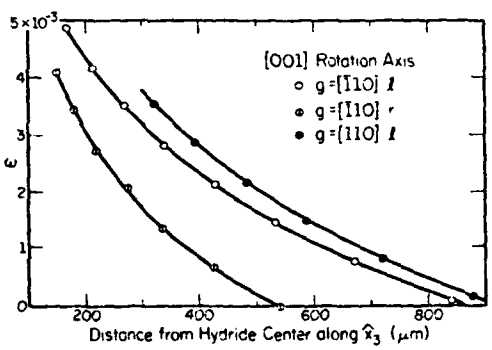

Fig. 3 Cumulative rotation as a function of distance from the β-NbH precipitate center. The contours were obtained for diffraction from [$\bar{1}$10] and rotation about [001].

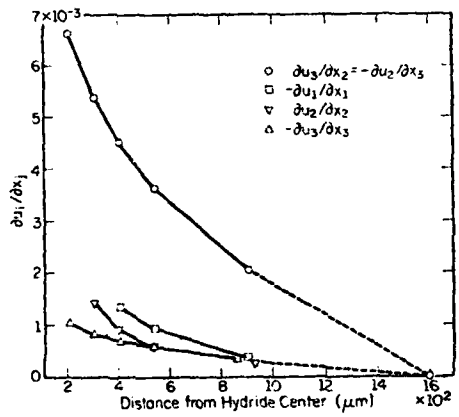

Fig. 4 Values of some of the $\partial u_i/\partial x_j$ along [$\bar{1}$10] from the center of the macroscopic β-NbH precipitate.

MEASUREMENT OF STRAIN TENSOR COMPONENTS ABOUT A β-NIOBIUM HYDRIDE PRECIPITATE

The Nb-H system provides a paradigm for hydrogen related failure via stress assisted nucleation and fracture of hydride precipitates. Precipitation of β-NbH and the accommodation of the accompanying 12% volume increase has been investigated by electron microscopy[3,4] and with optical and scanning electron microscopy[5]. The contour analysis described above is suited to determination of the deformation near the hydrides and will be applied below to obtain some of the components of strain.

Hydride precipitates were grown during cooling from room temperature in a thermal gradient in a $NbH_{0.03}$ single crystal having a thickness of 75 μm. Many small hydride precipitates formed at the colder end while larger, well spaced precipitates grew in the warmer portions of the crystal. The hydride precipitates remained on warming to room temperature because of the considerable hysteresis in the reversion[5]. Lang topographs, taken with Mó K_α radiation were used to select an isolated precipitate for the analysis.

Equi-inclination contours about the precipitate were obtained using reflection and transmission topography for rotations about $[\bar{1}10]$ and [001] axes. The equi-inclination contours in the $\underline{g}$ = [002] topograph of Fig. 2, plate 0, were produced by multiple exposure with rotations about the $[\bar{1}10]$ axis of 210 seconds of arc between contours. Deflection of contours between neighboring precipitates clearly shows the long range interaction of the strain fields which appear to extend two or three millimeters from the hydride plates. The appearance of interacting contours is somewhat similar to photoelastic contours observed about model precipitates with a similar volume expansion[5]. It is notable that precipitates with a large number of contours, particularly B and D, are those which have a pair of parallel dendritic arms and, hence, greater volume expansion. Figure 2, a composite of single exposure topographs with rotation axis $[\bar{1}10]$ and diffraction vector $\underline{g}$ = [002], shows the positions of the contours at 140 arc second increments of rotation. The magnitude of deformation at precipitate B is clearly evident; the area beside the precipitate is diffracting at angles greater than 0.3° from the orientation at which diffraction would occur if no hydride were present. The sense of rotation for the deformation field of the precipitate is opposite to that of the macroscopic curvature of the crystal.

Figure 3 shows the cumulative rotation vs. distance from the center of the precipitate for equi-inclination contours about the midpoint of precipitate B for the rotation axis [001]. The rotation angles are measured relative to the angle at which the contours from the precipitate merge with contours reflecting the general macroscopic curvature of the crystal. This position is the point at

which the contributions from the precipitate and the uniform curvature of the entire crystal cancel. The position corresponding to zero strain from the precipitate is that at which the uniform bending contours are no longer deflected by the field of the precipitate. Extrapolation to zero strain is necessary to obtain the magnitude of the strain component $\partial u_i/\partial x_j$ at a given position. An estimate of the strain between the last contour and the reference position is obtained by extrapolating $(\Delta\partial u_i/\partial x_j)/(\Delta\partial u_i/\partial x_{j\neq i})$ (measured between the last two contours) to zero strain. Fig. 4 presents estimates of some of $\partial u_i/\partial x_j$ along the line $\underline{x}_i = 0$. The results of Fig. 4 were based on contour positions on opposite sides of precipitate B taken with the same diffraction vector, $\underline{g} = [\bar{1}10]$; and the shear and dilational terms contribute as if the measurements were for $\pm\ h_i$, on the same side of the precipitate.

A major difficulty in the analysis near hydrides results from the complex hydride shapes; it is difficult to identify the "center" of the deformation. While the indistinct double image of precipitate B in the $\underline{g} = [002]$ topographs corresponds closely with the pair of parallel dendritic arms seen in optical and scanning electron micrographs, it is very difficult to identify the gross precipitate morphology. Therefore the origin from which to compare the equi-inclination contours from different reflections is difficult to determine. The use of white radiation and absorption edge contours will minimize this difficulty since images are obtained from the entire crystal. Fig. 5 shows a set of absorption edge contours of a lightly deformed niobium crystal which was produced with diffraction vector $\underline{g} = [002]$ and 90 arc seconds

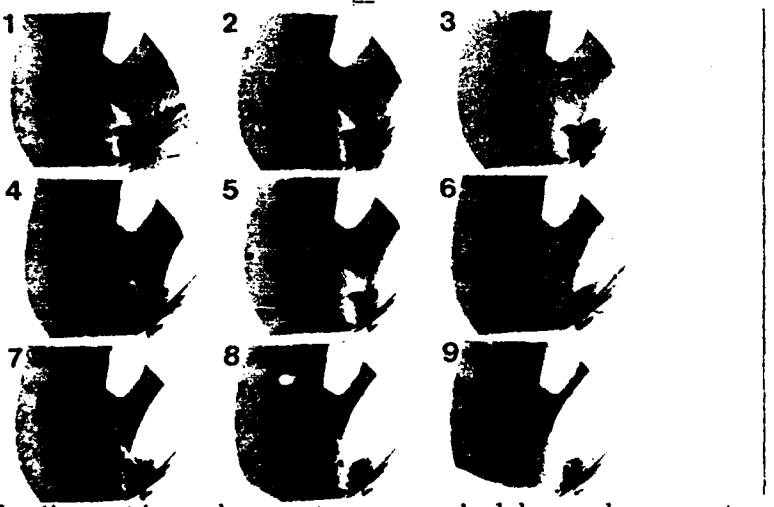

Fig. 5 Absorption edge contours, marked by a sharp contrast change, from a slightly deformed niobium crystal. (Data were taken at Daresbury Synchrotron Radiation Source in collaboration with S.T. Davies and D.K. Bowen.)

Reproduced from best available copy.

rotation between topographs[7]. The exposure of the Ilford L4 nuclear emulsion plates was chosen so that either side of the absorption edge, heavily or lightly absorbing, could be reproduced in good contrast.

The inter-contour spacings from any single reflection are much more reliable than comparisons between reflections since the reference position, that of the precipitate image, will vary little for the rotations used. This can be seen from Fig. 3 where there is little deviation of the individual points from the average curves. Because the difference of the displacement distance derivatives determine the contour spacings, the uncertainty of the origin from reflection to reflection makes the absolute magnitudes $\partial u_i/\partial x_j$ somewhat less reliable.

As described, the contour measurements may be used to characterize elastic strains. For plastically deformed specimens, the technique is only sensitive to the excess dislocation density, not to the total dislocation density.

ACKNOWLEDGEMENTS

This work was part of the Ph.D. thesis of S.R. Stock (Univ. of Illinois, 1983) and was supported by the Office of Naval Research through contract N00014-75-C-1012. One of the authors (SRS) would like to acknowledge support through an IBM graduate fellowship. We would also like to acknowledge use of the facilities of the MRL Center for Microanalysis of Materials which is supported as a national facility by the Materials Sciences Division of the Department of Energy.

REFERENCES

1. M. Hart, Bragg angle measurement and mapping, J. Cryst. Growth 55: 409 (1981).
2. U. Bonse and I. Hartmann, X-ray Measurement of Minute Lattice Strain in Perfect Silicon Crystals, Z. Kristall. 156: 265 (1981).
3. B.J. Makenas and H.K. Birnbaum, Phase changes in the niobium-hydrogen system I: accommodation effects during hydride precipitation, Acta Metall. 28: 979 (1980).
4. T. Schober, The niobium-hydrogen system--an electron microscope study II. low-temperature structures, Phys. Stat. Sol (a) 30: 107 (1975).
5. H.K. Birnbaum, M.L. Grossbeck and M. Amano, Hydride precipitation in Nb and some properties of NBH, J. Less-Common Metals, 49: 357 (1976).
6. M.S. Rashid and T.E.Scott, The group VA hydrides: a new type of phase transformation?, J. Less Common Metals, 31: 377 (1973).
7. D.K. Bowen, S.R. Stock, M. Pantos, S.T. Davies, Haydn Chen and H.K. Birnbaum, Topographic EXAFS, to appear (1983).

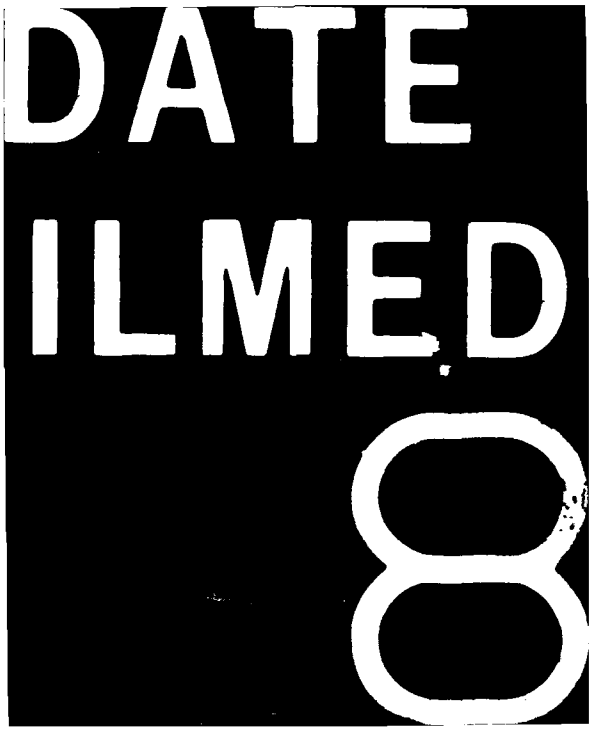
DATE
ILMED
8